Journal Pre-proof

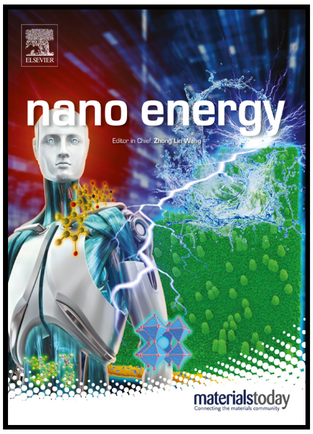

Triboelectric Nanogenerator and Artificial Intelligence to Promote Precision Medicine for Cancer

Meihua Chen, Yuankai Zhou, Jinyi Lang, Lijie Li, Yan Zhang

PII: S2211-2855(21)01032-6

DOI: https://doi.org/10.1016/j.nanoen.2021.106783

Reference: NANOEN106783

To appear in: *Nano Energy*

Received date: 22 September 2021
Revised date: 23 November 2021
Accepted date: 24 November 2021

Triboelectric Nanogenerator and Artificial Intelligence to Promote Precision Medicine for Cancer

Meihua Chen [1], Yuankai Zhou [1], Jinyi Lang [1], Lijie Li [2,*], and Yan Zhang [1,*]

[1] *Sichuan Cancer Hospital & Institute, Sichuan Cancer Center; Cancer Hospital affiliate to School of Medicine, School of Physics, University of Electronic Science and Technology of China, Radiation Oncology Key Laboratory of Sichuan Province, Chengdu 610054, China*

[2] *College of Engineering, Swansea University, Swansea, SA1 8EN, UK*

[*] To whom correspondence should be addressed, E-mail: zhangyan@uestc.edu.cn and L.Li@swansea.ac.uk

Abstract

The large-scale application of triboelectric nanogenerator (TENG) based self-powered devices holds promise for cancer treatment for millions of new cancer patients each year. TENG based sensors are capable of collecting patient data over a long time and provide precise cancer data sources for artificial intelligent process. TENG based devices possess great potential for targeted drug therapy, photodynamic therapy and electric field therapy on the tumor area based on the results of artificial intelligence analysis. This review summarizes and discusses the capabilities and prospects of TENG in cancer treatment, recovery, management, prevention and diagnosis. Cancer treatment and diagnosis are currently popular areas where TENGs with artificial intelligence has been applied in precision cancer research. TENGs with artificial intelligence based systems will be a potential candidate for applications in the field of cancer management and prevention.

Keywords:

Triboelectric nanogenerator; Precise medicine; Cancer; Self-powered sensor; Artificial intelligence

1. Introduction

In 2020, there were 19.3 million new cancer cases and nearly 10.0 million cancer deaths (9.9 million excluding nonmelanoma skin cancer) worldwide [1]. It is estimated that the number of new cancer cases in the world will reach 28.4 million in 20 years. Take lung cancer as an example, 30%-70% of patients will relapse with fatal diseases after surgical resection [2]. Environmental pollution and aging population make cancer the main cause of death in both more and less economically developed countries. Cancer treatment and recovery is a long-term process, metastasis and recurrence are the main causes of cancer death in human [3-5]. Timely diagnosis of tumor metastasis will affect morbidity and survival [6].

Improvements in the early diagnosis and treatment can significantly reduce the death rate of cancer, thus the death rate in the United States was 31% lower in 2018 than in 1991 [7]. The wearable, mobile sensor technologies have potential in promoting precision medicine and cancer drug development [8]. The food and drug administration (FDA) has issued guidelines on applications of wearables and mobile devices in cancer clinical care [8]. Physiological indicators, such as heart rate, blood sugar, oxygen saturation, etc. can be monitored after treatment to reflect the patient's status. In the medical industry, wearable devices are expected to collect information about the physiology, mental states and activities of a person to generate electronic health records [9-11]. For example, a mobile wearable device such as smartphone can be used to identify the status of patients after cancer treatment [12-15]. Recently, the wearable/implantable systems have identified early signs of an inflammatory response [16], and detected circulating tumor cells to identify cancer metastasis [17].

However, current mobile wearable devices face challenge of high battery replacement cost and waste batteries recycling problems. TENGs based sensors have the capability to harvest distributed energy for collecting distributed information from the environment [18]. The TENG/PENG based self-powered mobile wearable devices are good candidates for reducing energy consumption, batteries recycling and the maintenance cost of battery replacement [19-21]. In the last decade, with the rapid development of piezoelectric nanogenerator (PENG) [22] and triboelectric nanogenerator (TENG) [23] invented by Z. L. Wang, the nanogenerator (NG) based devices have been proven to hold a wide application prospect in many fields, especially in the medical and health field [24-27]. NG based self-powered sensors can harvest energy from the environment, such as human motion, mechanical vibration, hydroelectric power [28]. The NGs can be made by abundant low-cost and long-lasting materials, thus, the NGs were used as wearable/implantable sensors for long-term human health monitoring, as well as non-contact ambient sensors for Internet of Things (IoT) [29-32]. The lightweight, flexible, and biocompatible TENG/PENGs were designed as self-powered mobile wearable devices for patients [33, 34]. A self-powered magnet TENG based nanoscale drug delivery system (DDS) was developed in cancer research [35].

The uncertainty of the supply time of the environmental energy results in possible incompleteness of the data obtained by the self-powered sensor system. The developments of artificial intelligence (AI) can effectively recover the incomplete or short time information, which will overcome the data quality problem of self-powered sensor system. Although AI have made good progress in cancer diagnosis [36], large amounts of data collection are great challenge for cancer treatment, when people spend more time outside the hospital [37]. In practice, sensor data seldom provided the clinical characteristics of diagnosis or evaluation of the clinical situation, because many data of patients have been collected at normal conditions of the patients. Thus, among this large volume of data, clinical events worthy of attention are rare. TENG/PENG based data collection techniques for data collection across various phases can increase sample size and participants diversity, then improve clinical benefits and help conduct better modeling of diseases. There are three application relationships between AI algorithm and TENG based sensor [38]: first, AI algorithm analyzes TENG sensor data. Second, TENG sensor is used to design special AI sensor as the data source for AI algorithm. Finally, the special AI algorithm is designed for TENG based self-powered sensors. AI algorithm has been used in the clinical diagnosis and treatment of cancer [36]. At present, many works applied AI algorithms to process data generated at the hospitals, such as medical imaging [39-44] and biomarkers [45], etc.

For precision medicine in cancer, the development of wearable/implantable TENG/PENG and AI are key in timely data collection, data analysis, and feedback on the treatment, as shown in Figure 1. TENG/PENG based self-powered mobile wearable device has three possible applications in the cancer research. i) TENG as self-powered devices for cancer prevention, early diagnosis, precise treatment and management. ii) TENG based self-powered sensors both inside and outside the hospital for cancer. iii) TENG/PENG based self-powered mobile wearable devices for increasing the sample size and diversity of data. Thus, the precise diagnosis and treatment of cancer using AI based TENG self-powered system can be achieved.

2. Triboelectric Nanogenerators for Cancer Treatment

Battery replacement is inconvenient for patients, as it increases healthcare costs and may miss important medical data. The NGs can be the energy supply for sensors in precision medicine for cancer treatment, especially in flexible, wearable and implantable devices. As energy supplies, the NGs can power the various micro/nano actuators, such as the drug delivery, photodynamic, and electrical stimulation devices. The TENG based devices can reduce complications or injuries for drug delivery and photodynamic therapy [35, 46]. TENG has several advantages compared with previous methods: First, TENG can convert decentralized random mechanical energy into electric energy, avoiding the thermal effects that can be harmful to normal surrounding tissues when powered by wireless coils. TENG is a high voltage power supply that is easy to fabricate. Second, TENG is flexible, light-weight and miniaturized, suitable for long-term therapy process. The TENG based wearable device can continuously monitor physiological signal of human body. Third, TENG can be combined with AI to improve data quality, achieve long-term monitoring, analysis, feedback, and provide the full-process closed-loop cancer management [38]. TENGs is the preferred wearable and implantable energy source for precision medicine in cancer due to good biocompatibility. The precise delivery system of anti-tumor drugs can improve the tumor targeting ability and reduce the deleterious effects on normal cells. Current studies have made great progress in each field of TENGs and AI, but the complete precision medical system for cancer treatment has not yet demonstrated experimentally.

TENGs is used for controlling the drug release in the drug delivery system (DDS) that transports Doxorubicin (DOX) by red blood cells (RBCs) [35]. DOX is a chemotherapeutic drug commonly used to treat various solid tumors and hematopoietic tumors [47]. Due to

DOX lacking selectivity in tumor tissues, chemotherapy agents are often accompanied by severe side effects which limits efficacy and induces drug resistance. The novel magnet-TENG (MTENG) control the release of drugs in DOX loaded RBCs (D@RBCs) by collecting mechanical energy from the environment to generate electric field. Figure 2a presents the photo of MTENG and schematic diagram of MTENG deployed on a mouse. The electric field generated by the MTENG was delivered to the tumor site through the steel microneedles. Figure 2b shows the working principle of the NG-based DDS. After loading the DOX via hypotonic dialysis, the RBCs release the drug slowly. MTENG generates electric field to stimulates the RBCs, and the RBCs membrane forms nanopores, resulting in a significant increase in the release of DOX. When the electric field stimulation stops, the release of DOX returns to normal. Thus, the MTENG can be used to control the release of the drug from the DOX loaded RBCs (D@RBCs). To further study on the DDS in vivo, tumor samples from the mice were obtained after 30 days. As shown in Figures 2c and 2d, the METNG electric field stimulation significantly suppressed tumor growth and prolonged survival in the D@RBC group. Liu et al. proposed a TENG based self-powered electroporation system [48]. As shown in Figure 2e, the electric field is generated by TENG and then enhanced by the Ag NW-modified microfoam electrode. The electric field promotes the exogenous molecules to enter the cell. We speculate that this system could help deliver chemotherapy drugs to cancer cells. Liu et al. developed a TENG based electroporation system for transdermal drug delivery. As shown in Figure 2f, TENG converts biomechanical energy into pulsed electrical field. Nanoneedle-array on the skin of mice enhances local electric field to change membrane permeability and realizes electroporation drug delivery in vivo [49]. Ouyang et al. developed a TENG based self-powered transdermal drug delivery system [50]. The drug release dose can be tuned by changing the manual rotation time of TENG or the resistance in the power management system. Closed-loop devices can collect information about the patient state and take medical measures. Lee et al. developed a wearable patch for blood glucose monitoring and transdermal drug delivery to achieve closed-loop immediate treatment of diabetes [51]. The graphene-based device monitors blood glucose, when hyperglycemia is detected, the drug-loaded microneedles are triggered to release the drug into the blood. TENG based self-powered device is also very suitable for developing such a long-term monitoring and feedback treatment system.

Liu et al. designed a self-powered photodynamic therapy (PDT) system based on PENGs [46]. The biomechanical energy is harvested by the wearable twinning structure piezoelectric nanogenerator (ts-PENG) and transformed into electricity without external power supply, which can achieve long-term power supply for cancer treatment. PDT is a method of treating tumors with photosensitizers (PS) and specific wavelengths of light, which can be effectively powered by TENGs due to higher energy supply. The left part of Figure 2g shows the components of self-powered PDT (s-PDT) system and the upper right part shows the structure of ts-PENG. The schematic diagram of apoptosis induced by the combined action of PS and miniature light-emitting diode (m-LED) in the s-PDT system is shown in the lower right part of Figure 2g. Then the s-PDT was implanted into mice, and the body movement of mice drove the ts-PENG to generate electricity and light up the LED. Mice were injected with porphyrin to transfer the energy from LED. Figure 2h shows the change curve of tumor size in different experiment groups. The tumor inhibition rate in treatment regimen of LED+porphyrin group reached 87.46%.

Ma et al. proposed an Au/ZnO-based Trojan nanogenerators for tumor therapy [52]. As displayed in Figure 2i, researchers integrate the ZnO based nanogenerators with gold nanozymes, and modify them with biocompatible polyethylene glycol (PEG) and mitochondrial targeting peptides (MLS) to form the therapeutic platform. Finally, the platform is wrapped by the homologous C6 cancer cell membrane (CCM) vesicles, which confers homologous targeting and immune escape ability to the platform (MP-Au/ZnO@CCM for short, hereinafter). After entering the target cells, the platform is released from the vesicle. The ZnO based nanogenerator can generate nanoscale piezoelectric polarization electric field under the action of ultrasonic (US) wave. The electric field can disturb the mitochondrial membrane potential by electrostimulation. At the same time, polarization electric field can enhance multiple nanozyme-like activities of gold nanozymes to kill the cancer cells. Figure 2j shows that MP-Au/ZnO@CCM under ultrasound drive can reduce the survival rate of C6 cancer cells to 17.40%, which is significantly lower than other control groups. The researchers tested the anti-tumor effect of MP-Au /ZnO@CCM in nude mice with C6 tumor in vivo. As shown in Figure 2k, compared with other groups, the tumor growth of mice treated with MP-Au/ZnO@CCM US was significantly inhibited in the first 6 days. After 14 days of treatment, the tumor inhibition rate achieved 67.10%.

TENG based electrical stimulator can be used for cancer therapy [53]. Cell membrane potential can regulate cell cycle and promote cell differentiation, migration and proliferation [53, 54]. In the electrophysiological analysis of many cancer cell types, cancer cells have a higher degree of depolarization than normal cells, and depolarized membrane potential can promote the proliferation of cancer cells. This unusual membrane potential could serve as a valuable clinical marker for detecting cancer cells. During cancer treatment, the artificial regulation of membrane potential can control and even inhibit the proliferation and metastasis of cancer cells.

The TENGs/PENGs have potential applications as key energy supplies in sensor units for self-powered drug delivery, PDT, and electrical stimulator. The complete precision medical cancer treatment system will include the energy supply, precision data sensing and analysis process unit. AI will act as data analysis process unit. Recently, Jie et al. have demonstrated an integrated device of triboelectric effect based nanosensor for detection of dopamine in the alkaline condition [55]. The dopamine can enhance the efficacies of commonly used anticancer drugs and might have a role as an antiangiogenic agent for the treatment of breast and colon cancer [56]. This novel device combined with TENG holds great potential for the determination of dopamine in cancer treatment. Sun Yat-sen University Cancer Center proposed a deep learning model for automatically delineating the gross tumor volume (GTV) of nasopharyngeal carcinoma, which is more sensitive to radiotherapy [43]. Accurate tumor target contouring based on AI can significantly increase the survival rate of patients.

3. Triboelectric Nanogenerators for Cancer Recovery

Cancer treatments include surgery and radiotherapy. Wound healing of surgical site is an important issue that influences quality of life for cancer patients [57-59]. Wound infections by pathogenic bacteria are significant medical problems that affect postoperative patients [60]. Favorable wound healing after curative surgical procedures is an essential issue for cancer recovery. TENG based devices are expected to help patients quickly recover postoperative scars and prevent infections caused by weakened immunity [61]. Postoperative recovery also affects the quality of life of cancer patients.

Self-powered electric stimulation system based on rotatory disc-shaped TENG (RD-TENG) can enhance the proliferation and migration of fibroblasts, as shown in Figure 3a. TENGs provide potential techniques for developing portable electric stimulation device on tissue remodeling and wound healing. As shown in Figure 3b, following 5-day RD-TENG stimulation, the migration of L929 cells was significantly faster than the ones in control group. The migration related genes expression was tested by quantitative reverse transcription PCR (qRT-PCR), the quantitative analysis of the results indicated that both fibroblast growth factor 2 and delta like non-canonical Notch ligand 1 were significantly up-regulated in the RD-TENG stimulated cells.

Du et al. proposed a TENG device with minocycline-loaded layered double hydroxides@Al film (MSETENG), which can accelerate the healing of infected wounds by electrical stimulation and drug release [62]. The TENG patch was deployed in the wound area of the mice, as shown in Figure 3c. The biomechanical force caused by the motion of the mice drove TENG to generate electric field to stimulate the wound area. At the same time, the electrode of the patch contacted the infected wounds to release antibacterial drugs. As shown in Figure 3d, the wound healing of MSETENG group mice was significantly faster than that of other groups with no infection occurred, and then the wound healed on the 10th day.

Jeong et al. designed a wearable ionic TENG (iTENG) patch that can be used to accelerate wound healing [63]. Figure 3e shows a schematic diagram of iTENG accelerating wound healing in mice. The iTENG generates an electric field in the wound area when the mouse exercises, which stimulates cell proliferation and migration, and promotes the secretion of cell growth factors in these areas. As shown in Figure 3f, the wound healing rate based on iTENG electrical stimulation was significantly faster than other groups, and the wound size reduced to 5% of the initial size after 14 days.

Most of the sensor devices require external power sources to function, which may limit their application for *in-vivo* cases. Biocompatible, biodegradable self-powered devices are ideal power sources for wearable and implantable devices. Zheng et al. designed a TENG device based on biodegradable materials to convert biomechanical energy into electrical energy [64]. After working in an animal body for a period, its material can be biodegraded and reabsorbed by the animal body without any adverse effects.

4. Triboelectric Nanogenerators for Cancer Management

A simple, low-cost, and easily deployable sensor enables large-scale respiration data collection to reduce problems associated with small number of samples. TENG based wearable breath sensor can harvest biokinetic energy from human chest and abdomen movements while breathing and provide continuous sensing signals [65]. TENGs can be used for human-machine interface (HMI) devices, which is a potential application for cancer management.

Peng et al. proposed a self-powered all-nanofiber e-skin (SANES). The SANES powered by TENG can be applied to monitor the respiration and diagnose obstructive sleep apnea-hypopnea syndrome (OSAHS) in real time. As shown in Figures 4a and 4b, the respiratory motion can be monitored via the sensing signals by the SANES attached on abdomen. Figure 4c shows the electrical signal features of three typical breathing states, which are normal, hypopnea, and apnea. According to different corresponding rate, interval time, and intensity of respiration motion, SANES can distinguish different respiratory states precisely.

Radiation is used for almost every cancer, and about half of cancer patients receive radiotherapy [66-68]. The respiratory motion of cancer patients can significantly affect the treatment accuracy in radiotherapy especially for lung or liver cancer [69]. Accurate breath monitoring allows real-time tracking of tumor location during treatment and provides useful information for cancer management [70]. The TENG sensor can recognize the different postures of the patients by analyzing their respiratory behaviors, and the patient can also use the breath-driven TENG device for HMI [71]. Figure 4d shows the structure of TENG device for HMI. When the air flows through the TENG, the contact-separation motion between the PET film and the copper electrode generates electricity. The electric output signals of TENG in normal breathing and deliberate breathing are presented in Figure 4e. According to electric output signals, the TENG can assists patients in HMI by distinguishing different respiratory types to control some electrical appliances (Figure 4f). Figure 4g shows a schematic diagram of the wireless HMI system.

A wearable sensor system with machine learning algorithm for continuously measuring the respiratory behaviors was proposed by Chen et al [72]. As shown in Figure 4h, researchers deployed two wearable wireless sensors to detect abdominal and chest respiration. Figure 4i is a schematic diagram of wearable sensor system recognizing four posture breathing behaviors of the subjects via sensor data. Data of different postural breathing behaviors was used to train the machine learning algorithm based on random forest classifier to predict the breathing posture of the subjects through the extracted features. Due to the small sample number of subjects in this experiment, whether the wearable sensor system can be applied to more people is uncertain.

5. Triboelectric Nanogenerators for Cancer Prevention

The Centers for Disease Control (CDC) classifies cancer as a chronic disease. Patients will spend more time outside hospital than in hospital, which constitutes challenges for postoperative cancer recovery and cancer management [37]. Continuous monitoring of patients can minimize the impact of cancer [73]. TENG sensor collects the patient's long-term physiological data to facilitate the cancer management for the patient.

NG based self-powered sensor can harvest energy from the environment, such as the energy of human movement, to reduce the dependence on the battery. NG with abundant materials benefiting from low-cost and long-lasting characteristics can be used as in a wearable/implantable sensor for long-term monitoring of human physiological indicators, and be cooperated with some non-contact ambient sensors to identify and manage cancer high-risk factors.

Due to the aging and growth of the population, and the adoption of unhealthy lifestyles such as lack of exercise and consumption of high-calorie foods, the number of global cancer cases may increase by 60% in the next two decades [74]. Self-powered sensors and non-contact ambient sensors can be applied to reduce potentially modifiable risk factors and prevent cancer. For example, the low, medium, high, and extremely high levels of ultraviolet radiation (UVR) are defined by World Health Organization (WHO) [75, 76]. Exposure to high-intensity UVR causes skin cancer [77]. The self-powered sensor system can be used as a photodetector to convert UVR into electrical signal and provide early warning to people exposed to high-intensity UVR. The changes of UVR intensity can linearly regulate the output of TENG [76, 78, 79]. The prevention and reduction of high-risk factors in lifestyle, and better environment can effectively reduce the morbidity and mortality of cancer.

Lin Z.-H., et al. prepared UVR photodetector by using chemical bath deposition method to synthesize 3D Dendritic TiO_2 nanostructures, which can also be used as TENG [78]. Figure 5a shows the fabrication process of the TENG based self-powered UVR photodetector. Figure 5b shows that the output current is linearly positively correlated with power intensities of UVR light. An electrospun nanowires based TENG (ENTENG) was proposed by Zheng et al [76]. The ENTENG can supply energy for self-powered UVR level detection device. As shown in Figure 5c, the naturally bent Kapton films are connected to form an arch-shaped structure, that is a TENG structure with contact separation mode [20]. The structure of the self-powered UVR level detection device is shown in Figure 5d. As the UVR intensity rises, the current flowing through the UVR sensor gradually enhances (Figure 5e), lighting more flickering LEDs. This implies that the number of flickering LEDs is positively related to the UVR level.

Ethanol is a biomarker for lung cancer and liver cirrhosis [80-83], as well as a potential marker of head and neck tumors [84]. Volatile organic compounds (VOCs) in exhaled gas can be used to detect gastrointestinal cancer [85]. TENG based sensor can detect VOCs such as ethanol through exhaled gas [86, 87]. Wen et al. proposed a blow-driven TENG (BD-TENG) based active alcohol detector [86]. The structure of BD-TENG is shown in Figure 6a. Figure 6b shows the output voltage in relation with different alcohol concentrations and the composition of the self-powered breath analyzer. The BD-TENG generates electricity by the air flow propelling the blades. When there is alcohol in the air flow, the resistance of the sensor will be changed, so that the alarm can be triggered. Meng et al. improved the response of the ethanol sensor through TENG enhanced Schottky sensor [87]. As shown in Figure 6c, the output voltage generated by TENG is rectified and applied to the ZnO nano/microwire sensor. The response values of the ZnO ethanol sensor and the TENG treatment sensor increase as the ethanol concentration increases (Figure 6d). Compared with the original ZnO ethanol sensor, the sensor after TENG treatment has improved response and recovery time (Figure 6e). Zhang et al. designed a self-powered active sensor based on TENG made of different polymer films (Figure 6f), the sensor can detect liquid/gaseous water and ethanol [88]. The output signal decreases with the rise of ethanol concentration, and the decline is log-linear (Figure 6g).

The steady increase in the number of people diagnosed with cancer highlights the urgent need for expansion of cancer-prevention efforts. Eating habits, foods, and nutrition rank high among the most-important determinants of human cancer risks [89]. Cancer deaths may be related to dietary factors [90], such as the diet based on fatty foods and red meat, while relative small fruits and vegetables intake will increase the risk of cancer [91]. The pathogenic link between diet and cancer is not yet clear [92], but it is estimated that appropriate lifestyle and dietary measures can prevent cancer [93]. Deep learning technology can automatically classify daily food [94], which will help high-risk population and patients determine a healthy diet plan.

Food spoilage such as aflatoxin and high doses of nitrite may be the carcinogen or co-carcinogen [95-99]. Fungal spoilage of food can produce aflatoxin. The World Cancer Research Fund (WCRF) appraised that aflatoxin can increase the risk of liver cancer [100]. Accurate detection of food spoilage can effectively prevent food-borne diseases, including cancer. Cai et al. proposed a TENG-based wireless gas sensor system (TWGSS) for food-quality assessment [101]. Figure 7a shows the structure and working principle of TWGSS. The output voltage of TENG will decrease when ammonia is present in the air (Figure 7b). Figure 7c shows that the plot of voltage variation of TENG is linearly positively correlated with ammonia concentration, and better selectivity of the TWGSS for ammonia. The TWGSS can assess food quality by detecting the ammonia content in food. TENG based self-powered gas sensor and machine learning algorithm are combined to form an electronic nose system, which can identify spoilage odor in food. The working principle of biological olfactory system is that the nose acts as a gas sensor to collect gas data and transmit it to the brain for processing. According to the above principles, the electronic nose was designed as shown in Figure 7d [102]. The researchers established a spoiled food mixed odor dataset (Dataset-1) and a rotten fruit odor dataset (Dataset-2). These sensor signals are recognized as odor classification by establishing a convolutional spiking neural network with skip connections (RCSNN) model. Figure 7e shows the performance difference between RCSNN-12, 1D-DCNN, and ResNet-18 in dataset-1 and dataset-2. As we can see from the Figure 7e, the RCSNN proposed by the researcher has higher accuracy than the 1D-DCNN and is lighter than ResNet-18. The machine learning algorithm has the potential to combine with TENG sensor into a smart electronic nose system with self-powered edge calculation function. Lam et al. designed a total volatile organic compounds sensor powered by radio frequency radiation to monitor the food quality (Figure 7f) [103]. The trained machine learning algorithm is used to process the signals from the sensors and predict the state of food quality.

Insufficient physical activity can increase the risk of cancer [104]. In 2014, 46,300 patients suffered from cancer due to insufficient exercise. Exercise can reduce cancer incidence and the risk of recurrence. Outdoor air pollution has numerous adverse effects on human health, hundreds of thousands of people worldwide die of lung cancer every year due to PM air pollution [105]. Particulate matter (PM) and outdoor air pollution are carcinogenic [106-108]. In 2017, the global proportion of lung cancer deaths caused by PM2.5 air pollution in the outdoor environment reached 14% [1]. Cancer could be effectively prevented by reducing exposure to air pollution. TENG can generate a strong electric field to remove PM and volatile organic compounds (VOCs) in ambient atmosphere [109-115]. Gu et al. designed a high efficiency rotating TENG to charge the polyimide (PI) nanofiber film for filtering the PM in the air [109], and the device structure is shown in the Figure 8a. When the diameter of PM is about 15 to 550 nm, the average removal efficiency of TENG enhanced PI filter is about 80% (red line in Figure 8b), which is significantly higher than that of PI filter only (green line in Figure 8b). The removal efficiency of the PI filter and the TENG enhanced PI filter is nearly 100% for PM with the diameter of 0.54 to 20 μm (Figure 8c). Formaldehyde is an air pollutant that can cause many diseases. Feng et al. proposed a TENG-enhanced photocatalytic formaldehyde filter [110]. TENG provided an electric field for the photocatalyst-coated stainless steel filter to achieve the electrostatic adsorption effect and enhance the photocatalytic effect. The electric field provided by the TENG improved the formaldehyde degradation efficiency of the filter (Figure 8d). Automobile exhaust is one of the main pollution sources [111]. Han et al. proposed a self-powered triboelectric filter to reduce the content of PM in automobile exhaust. The triboelectric field generated by the triboelectric filter vibrates to remove PM from automobile exhaust, so the entire device does not require an external power. Figure 8e shows the top view structure of triboelectric filter. The deflector is set in the device to increase the length of gas filtering in the device to improve space utilization. The researchers tested the triboelectric filter on a vehicle tailpipe. Figure 8f presents the efficiency curves of the device, which shows that PM2.5 can be removed over ~95.5% at different working modes of the automobile. The pie charts of Figure 8f represent the percentages of different kinds of PMs in automobile exhaust. Liu et al. proposed a respiration TENG (R-TENG) driving self-powered electrostatic adsorption face mask (SEA-FM) [112]. The SEA-FM can effectively remove particulates continually through the electrostatic adsorption provided by the poly(vinylidene fluoride) electrospun nanofiber film (PVDF-ESNF) based R-TENG collection of respiratory energy. Figure 8g shows the working process of the R-TENG. On the expiratory state, the PVDF-ESNF and Cu film in the R-TENG contact and close the intake channel, and the airflow is forced out through the exhaust channel. On the inspiration state, the exhaust channel closed and the two films in the TENG separate to generate an electric field that can absorbs particles in the airflow. Figure 8h shows the removal efficiency curves of the PVDF-ESNF and R-TENG. The average removal efficiency of R-TENG is about twice that of PVDF-ESNF, and the removal efficiency of R-TENG is also more stable.

6. Artificial Intelligence to Promote Precision Medicine for Cancer

Medical imaging technology plays a key role in cancer diagnosis [116]. Deep learning technology is a new computer-aided diagnosis tool [117-119] and can automatically establish the significant hierarchal relationships from medical imaging to cancer classification [39-42], automatic contouring of tumor [43], cancer origin prediction [39], and survival rate prediction [44]. Regular tumor screening can detect potential cancer patients at an early stage, and treatment is most effective at early stage of cancer, thereby improving the survival rate of patients [7, 120, 121].

The deep learning model can predict primary or metastatic of the tumor with high accuracy after training, and use minimal clinical information to predict the original site (Figure 9a) [39]. Microsatellite instability-high (MSI-H) tumors in gastrointestinal cancers usually respond well to immunotherapy with immune checkpoint inhibitors [122]. Kather et al. proposed a deep learning network that can predict the spatial patterns of MSI from the Haematoxylum and Eosin (H&E) histology slides [40]. The model consists of a convolutional neural network (CNN) based tumor detector (Figure 9b), and MSI versus microsatellite stability (MSS) classifier (Figure 9c). Chen et al. directly used whole-slide images (WSI) as the input of CNN, and only labelled each slide without slicing the image into patches for labeling [41]. The cancerous regions marked by the pathologists (Figure 9d) and the critical regions of the model visualized by the class activation map (CAM) technology (Figure 9e) were highly corresponding. The CAM results of the model can be used for automatic contouring of the tumor.

The AI assisted the oncologists to improve the accuracy of diagnostics and reduce the contouring time. In actual treatment, biomarkers are used to predict patient prognosis and discuss different treatment options [44]. Skrede et al. used a deep learning model to process (H&E) stained tumor tissue sections to classify the prognosis of patients. As shown in Figure 9f, the deep learning model is divided into two parts. The first part uses CNN to automatically outline cancer tissues, and the second part uses CNN to divide patients into three prognostic categories. This model performed better than the established molecular and morphological prognostic markers and may be used in decision making options for adjuvant treatment.

Tumor markers are biological or biochemical substances produced by tumor cells. Their concentration is related to tumor size, clinical stage and prognosis, and they play an important role in the tumor screening, diagnosis, targeted therapy and prognosis. Kim et al. developed a prostate cancer (PCa) screening technique based on urinary multimarker sensors and AI analysis [45]. The urinary multimarker sensor measures four different PCa biomarkers from urine to produce sensing signals. The machine learning algorithms process sensing signals to screen for PCa without the need for a digital rectal examination. Figure 9g is the schematic diagram of urinary multimarker sensors and AI analysis for PCa screening. Multiple biomarkers produced by PCa cells are diffused to the urethra and excreted in urine. The biomarkers in the urine react with four channels that contain different antibodies in the multimarker sensor to produce signals. Two machine learning algorithms, random forest and neural network, were used to process the sensing signals and predict whether a patient has the disease. The diagnostic accuracy of the algorithms improved with the increase of the number of biomarkers, and finally reached the accuracy of over 90%.

Sharma et al. report a single-walled carbon nanotubes (SWCNTs) based immunosensor to detect the osteopontin (OPN) that is the prostate cancer biomarker [123]. The immunosensor consisted of two Au/ITO electrodes on a glass substrate and SWCNTs deposited between the two electrodes by electrophoresis. Figure 9h shows the basic structure of the SWCNTs based immunosensor. Figure 9i shows the highly linear variation of the relative resistance of the immune sensor with OPNs concentration, and the curve also shows high selectivity of OPN to different concentrations of human serum and phosphate buffer saline (PBS). This type of immune sensor that reacts with cancer biomarker to produce characteristic output can be used as a development direction of self-powered sensors in the field of cancer diagnosis.

Conventional cancer diagnosis and treatment has been transformed into a multi-faceted, all-round, and full-course medical care and support for patients. Cancer has been regarded as a chronic disease. The treatment and recovery of cancer is a long-term process including continuous care, prevention and monitoring of patients [73]. AI is used for signal processing of medical images, mainly for cancer detection, cancer diagnosis and tumor tracing [124]. AI is mainly applied in medical imaging processing in cancer diagnosis and treatment, its training requires millions of data, especially labeled data. The AI model trained by multi-omics data can predict the prognosis of cancer patients and improves the treatment intervention for patients [125]. While the increasing complexity of cancer diagnosis and treatment in hospitals and outpatient facilities makes it difficult to access, identify, and extract all data by traditional manual methods [126]. This obstacle of data acquisition, especially continuous out-of-hospital data, leads to the lack of many key information during oncology care. Wearable/ medical devices can make conformal contact with the human body or tissue to collect electrophysiological signals and provide real-time medical data for monitoring the body state of cancer patients and their diagnosis and treatment, as well as help individuals pursue a healthier lifestyle. TENG based self-powered sensors are capable of collecting patient data over a long time and provide precision cancer data sources for AI process, and to promote positive behaviors through electronic self-reports, web-based consultation, and real-time feedback and monitoring various long-term medical conditions at home. There are three application relationships between AI algorithm and TENG based sensor [38]: first, AI algorithm analyzes TENG sensor data. Second, TENG sensor is used to design special AI sensor as the data source for AI algorithm. Finally, the special AI algorithm is designed for TENG based self-powered sensors. AI algorithm has been used in the clinical diagnosis and treatment of cancer [36].

In order to accurately assess the health status of users, long-time and continuous recording and tracking of molecular information is needed. Traditional clinical blood analysis is determined by invasive blood collection, which cannot offer continuous data [127]. TENGs and AI can form the system of the comprehensive processing of various continuous and long-term physiological signals for early screening.

TENG can be used as a biomarker sensor to collect data information on blood [128, 129], sweat [130], urine [131] and respiratory components [86-88]. TENG sensors have the following advantages compared to traditional sensors: First, TENG can convert decentralized random mechanical energy into electric energy, avoiding the thermal effects that can be harmful to normal surrounding tissues when powered by wireless coils. TENG is a high voltage power supply that is easy to fabricate. Second, TENG is flexible, light-weight and miniaturized, suitable for long-term therapy process. It could be used as a wearable device to regularly or continuously monitor physiological signal of human body for generating long-term data and timely monitor abnormalities.

7. Challenges and Potential Application for Triboelectric Nanogenerators in Cancer

This review summarizes the potential application of TENG in cancer treatment, recovery, management and prevention. AI method specifically deep learning algorithm can be used for cancer diagnosis. The TENG based mobile wearable devices with low-cost, maintenance-free and increased comfort are ideal application for large-scale deployment in cancer patients for monitoring the physical status. The AI algorithm can analyze the medical data collected by TENG based devices. TENG based devices can be used as a data source for AI, which can also be used for cancer treatment based on AI decisions. The combination of self-powered devices and AI algorithms is essential for future precision medical in cancer diagnosis and treatment. In the future, TENG powered AI systems that assist doctors to make treatment plan, estimate treatment efficacy, and predict the development trend of tumor.

AI algorithms are currently widely used in cancer diagnosis, and TENG based self-powered devices are gradually applied in cancer treatment. There are some potential development directions of integrated TENG and AI devices in precision medicine for cancer treatment:

(1) Early screening and diagnosis of cancer are new and hot application areas of AI for TENG based sensors. The TENG based self-powered devices collect cancer clinical data as the data source for AI algorithms. TENG based self-powered sensor has been used for gas sensor, and liquid composition analysis. TENG may be used to develop sensors for monitoring cancer biomarkers. AI algorithms have been used to process sensor data for cancer diagnosis.

(2) Another area of future development is the TENG/PENG based AI system for precision cancer treatment. TENG/PENG based devices have been used in targeted drug therapy, photodynamic therapy and electrical stimulation in cancer treatment. TENG/PENG can harvest energy from the body such as breathing, joint movement and muscle stretching,

which could be used as a potential long-term treatment for cancer. To reduce pain, TENG/PENG based wearable and implantable devices need to be light, biocompatible and corrosion resistant. Targeted and programmable nanorobots based on TENG/PENG are also the research direction for cancer therapy.

(3) The large-scale TENG based devices for long-term monitoring of human physical data outside the hospital is another future research and development direction. Long-term and large-scale collection and processing of off-hospital data indicates the need for long-term stability, low-cost, maintenance-free, mobile, wearable and comfortable deployment of medical sensors, where TENG is suitable to meet the demand in this direction. Human body and environment can provide rich and random energy for TENG based self-powered devices, which fills the gap in data collection and analysis of non-clinical cancer outside the hospital. TENG based sensor collects data by random energy, at same time, AI recovers and analyzes the data to determine whether the current patient is at risk of cancer or whether the cancer prognosis is positive or not. The specific segment of the data determines the prediction result, and the AI algorithm needs to extract decision-making features from the long-term random data.

(4) The TENG based AI system for cancer research will be a future direction. Recurrence and metastasis are the main causes of cancer deaths, so long-term data collection inside and outside the hospital and long-term cancer treatment system in cancer screening, diagnosis, treatment and recovery are very important. The data from TENG based sensors provide novel diagnosis and treatment characteristics, how to analyze the data is an open question for current AI science and technology. Developing new AI method for TENG application in precision medical will provide a good opportunity for early diagnosis, treatment, recovery and cure. AI needs to develop new algorithms that are more suitable for TENG devices to improve the real-time performance of diagnosis and screening. TENG devices and AI algorithm based cancer diagnosis and treatment system is expected to form closed loop system: TENG sensor collects patient data and analyzes it by AI algorithms, and then controls the TENG treatment devices to release drugs, which may effectively treat cancer in the future.

Acknowledgements

The authors are thankful for the support from University of Electronic Science and Technology of China (ZYGX2015KYQD063), Swansea University, SPARC II project, and Thousand Talents program for a pioneer researcher and his innovation team, China.

References

1. Sung, H., et al., **Global Cancer Statistics 2020: GLOBOCAN Estimates of Incidence and Mortality Worldwide for 36 Cancers in 185 Countries**. CA: A Cancer Journal for Clinicians, 71 (3) (2021), pp. 209-249.
2. Murphy, D.J. and K.G. Blyth, **Predicting lung cancer recurrence from circulating tumour DNA. Commentary on 'Phylogenetic ctDNA analysis depicts early-stage lung cancer evolution'**. Cell Death & Differentiation, 24 (9) (2017), pp. 1473-1474.
3. Qin, L., et al., **A tumor-to-lymph procedure navigated versatile gel system for combinatorial therapy against tumor recurrence and metastasis**. Science Advances, 6 (36) (2020), pp. eabb3116.
4. Schroeder, A., et al., **Treating metastatic cancer with nanotechnology**. Nature Reviews Cancer, 12 (1) (2012), pp. 39-50.
5. Ebinger, S., et al., **Characterization of Rare, Dormant, and Therapy-Resistant Cells in Acute Lymphoblastic Leukemia**. Cancer cell, 30 (6) (2016), pp. 849-862.
6. Fathallah-Shaykh, H.M., et al., **Diagnosing growth in low-grade gliomas with and without longitudinal volume measurements: A retrospective observational study**. PLoS medicine, 16 (5) (2019), pp. e1002810.
7. Siegel, R.L., et al., **Cancer Statistics, 2021**. CA: a cancer journal for clinicians, 71 (1) (2021), pp. 7-33.

8. Cox, S.M., A. Lane, and S.L. Volchenboum, **Use of Wearable, Mobile, and Sensor Technology in Cancer Clinical Trials**. JCO Clinical Cancer Informatics, 2 (2018), pp. 1-11.

9. Dunn, J., et al., **Wearable sensors enable personalized predictions of clinical laboratory measurements**. Nature Medicine, 27 (6) (2021), pp. 1105-1112.

10. Strain, T., et al., **Wearable-device-measured physical activity and future health risk**. Nature Medicine, 26 (9) (2020), pp. 1385-1391.

11. Yetisen, A.K., et al., **Wearables in Medicine**. Advanced Materials, 30 (33) (2018), pp. 1706910.

12. Low, C.A., **Harnessing consumer smartphone and wearable sensors for clinical cancer research**. npj Digital Medicine, 3 (1) (2020), pp. 140.

13. Douma, J.A.J., H.M.W. Verheul, and L.M. Buffart, **Feasibility, validity and reliability of objective smartphone measurements of physical activity and fitness in patients with cancer**. BMC Cancer, 18 (1) (2018), pp. 1052.

14. Soto-Perez-De-Celis, E., et al., **A pilot study of an accelerometer-equipped smartphone to monitor older adults with cancer receiving chemotherapy in Mexico**. J Geriatr Oncol, 9 (2) (2018), pp. 145-151.

15. Panda, N., et al., **Using Smartphones to Capture Novel Recovery Metrics After Cancer Surgery**. JAMA Surg, 155 (2) (2020), pp. 123-129.

16. Li, X., et al., **Digital Health: Tracking Physiomes and Activity Using Wearable Biosensors Reveals Useful Health-Related Information**. PLOS Biology, 15 (1) (2017), pp. e2001402.

17. Kim, T.H., et al., **A temporary indwelling intravascular aphaeretic system for in vivo enrichment of circulating tumor cells**. Nature Communications, 10 (1) (2019), pp. 1478.

18. Wang, Z.L., **Entropy theory of distributed energy for internet of things**. Nano Energy, 58 (2019), pp. 669-672.

19. Pu, X., et al., **Ultrastretchable, transparent triboelectric nanogenerator as electronic skin for biomechanical energy harvesting and tactile sensing**. Science Advances, 3 (5) (2017), pp. e1700015.

20. Wu, C., et al., **Triboelectric Nanogenerator: A Foundation of the Energy for the New Era**. Advanced Energy Materials, 9 (1) (2019), pp. 1802906.

21. Wang, S., et al., **Molecular surface functionalization to enhance the power output of triboelectric nanogenerators**. Journal of Materials Chemistry A, 4 (10) (2016), pp. 3728-3734.

22. Wang, Z.L. and J. Song, **Piezoelectric Nanogenerators Based on Zinc Oxide Nanowire Arrays**. Science, 312 (5771) (2006), pp. 242.

23. Fan, F.-R., Z.-Q. Tian, and Z. Lin Wang, **Flexible triboelectric generator**. Nano Energy, 1 (2) (2012), pp. 328-334.

24. Wang, Z.L., T. Jiang, and L. Xu, **Toward the blue energy dream by triboelectric nanogenerator networks**. Nano Energy, 39 (2017), pp. 9-23.

25. Luo, J., W. Gao, and Z.L. Wang, **The Triboelectric Nanogenerator as an Innovative Technology toward Intelligent Sports**. Advanced Materials, 33 (17) (2021), pp. 2004178.

26. Alagumalai, A., et al., **Towards smart cities powered by nanogenerators: Bibliometric and machine learning–based analysis**. Nano Energy, 83 (2021), pp. 105844.

27. Wang, H., et al., **Triboelectric nanogenerators for human-health care**. Science Bulletin, 66 (5) (2021), pp. 490-511.

28. Wang, Z.L., J. Chen, and L. Lin, **Progress in triboelectric nanogenerators as a new energy technology and self-powered sensors**. Energy & Environmental Science, 8 (8) (2015), pp. 2250-2282.

29. Wang, Z.L., **Triboelectric Nanogenerator (TENG)—Sparking an Energy and Sensor Revolution**. Advanced Energy Materials, 10 (17) (2020), pp. 2000137.

30. Li, R., et al., **Smart Wearable Sensors Based on Triboelectric Nanogenerator for Personal Healthcare Monitoring**. 12 (4) (2021), pp. 352.

31. Yi, F., et al., **Recent Advances in Triboelectric Nanogenerator-Based Health Monitoring**. Advanced Functional Materials, 29 (41) (2019), pp. 1808849.

32. Wang, Z.L., **From contact electrification to triboelectric nanogenerators**. Reports on Progress in Physics, 84 (9) (2021), pp. 096502.

33. Liu, Z., et al., **Wearable and Implantable Triboelectric Nanogenerators**. Advanced Functional Materials, 29 (20) (2019), pp. 1808820.

34. Chen, C., et al., **Direct Current Fabric Triboelectric Nanogenerator for Biomotion Energy Harvesting**. ACS Nano, 14 (4) (2020), pp. 4585-4594.

35. Zhao, C., et al., **Highly Efficient In Vivo Cancer Therapy by an Implantable Magnet Triboelectric Nanogenerator**. Advanced Functional Materials, 29 (41) (2019), pp. 1808640.

36. Dlamini, Z., et al., **Artificial intelligence (AI) and big data in cancer and precision oncology**. Computational and Structural Biotechnology Journal, 18 (2020), pp. 2300-2311.

37. Haque, A., A. Milstein, and L. Fei-Fei, **Illuminating the dark spaces of healthcare with ambient intelligence**. Nature, 585 (7824) (2020), pp. 193-202.

38. Zhou, Y., et al., **Triboelectric nanogenerator based self-powered sensor for artificial intelligence**. Nano Energy, 84 (2021), pp. 105887.

39. Lu, M.Y., et al., **AI-based pathology predicts origins for cancers of unknown primary**. Nature, 594 (7861) (2021), pp. 106-110.

40. Kather, J.N., et al., **Deep learning can predict microsatellite instability directly from histology in gastrointestinal cancer**. Nature Medicine, 25 (7) (2019), pp. 1054-1056.

41. Chen, C.-L., et al., **An annotation-free whole-slide training approach to pathological classification of lung cancer types using deep learning**. Nature Communications, 12 (1) (2021), pp. 1193.

42. Chuang, W.-Y., et al., **Successful Identification of Nasopharyngeal Carcinoma in Nasopharyngeal Biopsies Using Deep Learning**. Cancers, 12 (2) (2020), pp. 507.

43. Lin, L., et al., **Deep Learning for Automated Contouring of Primary Tumor Volumes by MRI for Nasopharyngeal Carcinoma**. Radiology, 291 (3) (2019), pp. 677-686.

44. Skrede, O.-J., et al., **Deep learning for prediction of colorectal cancer outcome: a discovery and validation study**. The Lancet, 395 (10221) (2020), pp. 350-360.

45. Kim, H., et al., **Noninvasive Precision Screening of Prostate Cancer by Urinary Multimarker Sensor and Artificial Intelligence Analysis**. ACS Nano, 15 (3) (2021), pp.

4054-4065.

46. Liu, Z., et al., **Human Motion Driven Self-Powered Photodynamic System for Long-Term Autonomous Cancer Therapy**. ACS Nano, 14 (7) (2020), pp. 8074-8083.

47. Ma, Z.-G., et al., **Toll-like receptor 5 deficiency diminishes doxorubicin-induced acute cardiotoxicity in mice**. Theranostics, 10 (24) (2020), pp. 11013-11025.

48. Liu, Z., et al., **High-Throughput and Self-Powered Electroporation System for Drug Delivery Assisted by Microfoam Electrode**. ACS Nano, 14 (11) (2020), pp. 15458-15467.

49. Liu, Z., et al., **Self-Powered Intracellular Drug Delivery by a Biomechanical Energy-Driven Triboelectric Nanogenerator**. Advanced Materials, 31 (12) (2019), pp. 1807795.

50. Ouyang, Q., et al., **Self-powered, on-demand transdermal drug delivery system driven by triboelectric nanogenerator**. Nano Energy, 62 (2019), pp. 610-619.

51. Lee, H., et al., **A graphene-based electrochemical device with thermoresponsive microneedles for diabetes monitoring and therapy**. Nature Nanotechnology, 11 (6) (2016), pp. 566-572.

52. Ma, K., et al., **Ultrasound-activated Au/ZnO-based Trojan nanogenerators for combined targeted electro-stimulation and enhanced catalytic therapy of tumor**. Nano Energy, 87 (2021), pp. 106208.

53. Conta, G., et al., **Triboelectric Nanogenerators for Therapeutic Electrical Stimulation**. Advanced Materials, 33 (26) (2021), pp. 2007502.

54. Liu, Z., et al., **Electroactive Biomaterials and Systems for Cell Fate Determination and Tissue Regeneration: Design and Applications**. Advanced Materials, 33 (32) (2021),

pp. 2007429.

55. Jie, Y., et al., **Self-Powered Triboelectric Nanosensor with Poly(tetrafluoroethylene) Nanoparticle Arrays for Dopamine Detection**. ACS Nano, 9 (8) (2015), pp. 8376-8383.

56. Sarkar, C., et al., **Dopamine Increases the Efficacy of Anticancer Drugs in Breast and Colon Cancer Preclinical Models**. Clinical Cancer Research, 14 (8) (2008), pp. 2502.

57. Giano, M.C., et al., **Injectable bioadhesive hydrogels with innate antibacterial properties**. Nature Communications, 5 (1) (2014), pp. 4095.

58. Isaac, D.L., **Complex Wound Management Using Negative Pressure Wound Therapy With Instillation and Dwell Time in a Cancer Care Setting**. Wounds : a compendium of clinical research and practice, 32 (5) (2020), pp. 118-122.

59. De Rooij, L., et al., **Negative pressure wound therapy does not decrease postoperative wound complications in patients undergoing mastectomy and flap fixation**. Scientific Reports, 11 (1) (2021), pp. 9620.

60. Petruk, G., et al., **Concentration- and pH-Dependent Oligomerization of the Thrombin-Derived C-Terminal Peptide TCP-25**. Biomolecules, 10 (11) (2020), pp. 1572.

61. Hu, W., et al., **Enhancing proliferation and migration of fibroblast cells by electric stimulation based on triboelectric nanogenerator**. Nano Energy, 57 (2019), pp. 600-607.

62. Du, S., et al., **Surface-engineered triboelectric nanogenerator patches with drug loading and electrical stimulation capabilities: Toward promoting infected wounds healing.** Nano Energy, 85 (2021), pp. 106004.

63. Jeong, S.-H., et al., **Accelerated wound healing with an ionic patch assisted by a triboelectric nanogenerator**. Nano Energy, 79 (2021), pp. 105463.

64. Zheng, Q., et al., **Biodegradable triboelectric nanogenerator as a life-time designed implantable power source**. Science Advances, 2 (3) (2016), pp. e1501478.

65. Peng, X., et al., **All-Nanofiber Self-Powered Skin-Interfaced Real-Time Respiratory Monitoring System for Obstructive Sleep Apnea-Hypopnea Syndrome Diagnosing**. Advanced Functional Materials, 31 (34) (2021), pp. 2103559.

66. Chandra, R.A., et al., **Contemporary radiotherapy: present and future**. The Lancet, 398 (10295) (2021), pp. 171-184.

67. Bentzen, S.M., et al., **Towards evidence-based guidelines for radiotherapy infrastructure and staffing needs in Europe: the ESTRO QUARTS project**. Radiotherapy and Oncology, 75 (3) (2005), pp. 355-365.

68. Perni, S., et al., **Assessment of Use, Specificity, and Readability of Written Clinical Informed Consent Forms for Patients With Cancer Undergoing Radiotherapy**. JAMA Oncology, 5 (8) (2019), pp. e190260-e190260.

69. Oh, Y., et al., **Design and Evaluation of a MEMS Magnetic Field Sensor-Based Respiratory Monitoring and Training System for Radiotherapy**. Sensors, 18 (9) (2018), pp. 2742.

70. Gu, C., et al., **Accurate Respiration Measurement Using DC-Coupled Continuous-Wave Radar Sensor for Motion-Adaptive Cancer Radiotherapy**. IEEE Transactions on Biomedical Engineering, 59 (11) (2012), pp. 3117-3123.

71. Zhang, B., et al., **Breath-based human–machine interaction system using triboelectric**

nanogenerator. Nano Energy, 64 (2019), pp. 103953.

72. Chen, A., et al., **Machine-learning enabled wireless wearable sensors to study individuality of respiratory behaviors**. Biosensors and Bioelectronics, 173 (2021), pp. 112799.

73. Phillips, J.L. and D.C. Currow, **Cancer as a chronic disease**. Collegian, 17 (2) (2010), pp. 47-50.

74. Chen, W., et al., **Disparities by province, age, and sex in site-specific cancer burden attributable to 23 potentially modifiable risk factors in China: a comparative risk assessment**. The Lancet Global Health, 7 (2) (2019), pp. e257-e269.

75. Organization, W.H. and I.C.o.N.-I.R. Protection, *Global solar UV index: a practical guide*. 2002, World Health Organization: Geneva, Switzerland.

76. Zheng, Y., et al., **An electrospun nanowire-based triboelectric nanogenerator and its application in a fully self-powered UV detector**. Nanoscale, 6 (14) (2014), pp. 7842-7846.

77. Narayanan, D.L., R.N. Saladi, and J.L. Fox, **Review: Ultraviolet radiation and skin cancer**. International Journal of Dermatology, 49 (9) (2010), pp. 978-986.

78. Lin, Z.-H., et al., **Triboelectric Nanogenerator as an Active UV Photodetector**. Advanced Functional Materials, 24 (19) (2014), pp. 2810-2816.

79. Cheng, G., et al., **Managing and maximizing the output power of a triboelectric nanogenerator by controlled tip–electrode air-discharging and application for UV sensing**. Nano Energy, 44 (2018), pp. 208-216.

80. Dent, A.G., T.G. Sutedja, and P.V. Zimmerman, **Exhaled breath analysis for lung**

cancer. Journal of thoracic disease, 5 (Suppl 5) (2013), pp. S540-S550.

81. Su, Y., et al., **Self-Powered Respiration Monitoring Enabled By a Triboelectric Nanogenerator**. Advanced Materials, 33 (35) (2021), pp. 2101262.

82. Jones, A.W., **Ethanol metabolism in patients with liver cirrhosis**. Journal of Clinical Forensic Medicine, 7 (1) (2000), pp. 48-51.

83. Liao, Y.S., et al., **Assessment of liver cirrhosis for patients with Child's A classification before hepatectomy using dynamic contrast-enhanced MRI**. Clinical Radiology, 74 (5) (2019), pp. 407.e11-407.e17.

84. Gruber, M., et al., **Analysis of exhaled breath for diagnosing head and neck squamous cell carcinoma: a feasibility study**. British Journal of Cancer, 111 (4) (2014), pp. 790-798.

85. Amal, H., et al., **Detection of precancerous gastric lesions and gastric cancer through exhaled breath**. Gut, 65 (3) (2016), pp. 400.

86. Wen, Z., et al., **Blow-driven triboelectric nanogenerator as an active alcohol breath analyzer**. Nano Energy, 16 (2015), pp. 38-46.

87. Meng, J., et al., **Triboelectric Nanogenerator Enhanced Schottky Nanowire Sensor for Highly Sensitive Ethanol Detection**. Nano Letters, 20 (7) (2020), pp. 4968-4974.

88. Zhang, H., et al., **Triboelectric nanogenerator as self-powered active sensors for detecting liquid/gaseous water/ethanol**. Nano Energy, 2 (5) (2013), pp. 693-701.

89. Key, T.J., et al., **The effect of diet on risk of cancer**. The Lancet, 360 (9336) (2002), pp. 861-868.

90. Willett, W.C., **Diet, nutrition, and avoidable cancer**. Environmental Health

Perspectives, 103 (suppl 8) (1995), pp. 165-170.

91. Ferguson, L.R., **Meat and cancer**. Meat Science, 84 (2) (2010), pp. 308-313.

92. Xia, S., et al., **Prevention of Dietary-Fat-Fueled Ketogenesis Attenuates BRAF V600E Tumor Growth**. Cell Metabolism, 25 (2) (2017), pp. 358-373.

93. Donaldson, M.S., **Nutrition and cancer: a review of the evidence for an anti-cancer diet**. Nutrition journal, 3 (2004), pp. 19.

94. Hu, L., et al. **Automatic Diet Recording Based on Deep Learning**. 2018 Chinese Automation Congress (CAC), IEEE, 2018, pp. 3778-3782.

95. Liu, Y. and F. Wu, **Global Burden of Aflatoxin-Induced Hepatocellular Carcinoma: A Risk Assessment**. Environmental Health Perspectives, 118 (6) (2010), pp. 818-824.

96. Havelaar, A.H., et al., **World Health Organization Global Estimates and Regional Comparisons of the Burden of Foodborne Disease in 2010**. PLOS Medicine, 12 (12) (2015), pp. e1001923.

97. Kerekes, E.B., et al., **Anti-Biofilm Effect of Selected Essential Oils and Main Components on Mono- and Polymicrobic Bacterial Cultures**. Microorganisms, 7 (9) (2019), pp. 345.

98. Schweinsberg, F. and V. Bürkle, **Nitrite: A Co-carcinogen?** Journal of Cancer Research and Clinical Oncology, 109 (3) (1985), pp. 200-202.

99. Cammack, R., et al., **Nitrite and nitrosyl compounds in food preservation**. Biochimica et Biophysica Acta (BBA) - Bioenergetics, 1411 (2) (1999), pp. 475-488.

100. Mayne, S.T., M.C. Playdon, and C.L. Rock, **Diet, nutrition, and cancer: past, present and future**. Nature Reviews Clinical Oncology, 13 (8) (2016), pp. 504-515.

101. Cai, C., et al., **Integration of a porous wood-based triboelectric nanogenerator and gas sensor for real-time wireless food-quality assessment**. Nano Energy, 83 (2021), pp. 105833.

102. Xiong, Y., et al., **An Odor Recognition Algorithm of Electronic Noses Based on Convolutional Spiking Neural Network for Spoiled Food Identification**. Journal of The Electrochemical Society, 168 (7) (2021), pp. 077519.

103. Lam, M.B., T. Nguyen, and W. Chung, **Deep Learning-Based Food Quality Estimation Using Radio Frequency-Powered Sensor Mote**. IEEE Access, 8 (2020), pp. 88360-88371.

104. Xie, S.-H. and J. Lagergren, **Risk factors for oesophageal cancer**. Best Practice & Research Clinical Gastroenterology, 36-37 (2018), pp. 3-8.

105. Turner, M.C., et al., **Outdoor air pollution and cancer: An overview of the current evidence and public health recommendations**. CA: A Cancer Journal for Clinicians, 70 (6) (2020), pp. 460-479.

106. Raaschou-Nielsen, O., et al., **Air pollution and lung cancer incidence in 17 European cohorts: prospective analyses from the European Study of Cohorts for Air Pollution Effects (ESCAPE)**. The Lancet Oncology, 14 (9) (2013), pp. 813-822.

107. Valavanidis, A., K. Fiotakis, and T. Vlachogianni, **Airborne Particulate Matter and Human Health: Toxicological Assessment and Importance of Size and Composition of Particles for Oxidative Damage and Carcinogenic Mechanisms**. Journal of Environmental Science and Health, Part C, 26 (4) (2008), pp. 339-362.

108. Hamra Ghassan, B., et al., **Outdoor Particulate Matter Exposure and Lung Cancer: A**

Systematic Review and Meta-Analysis. Environmental Health Perspectives, 122 (9) (2014), pp. 906-911.

109. Gu, G.Q., et al., **Triboelectric Nanogenerator Enhanced Nanofiber Air Filters for Efficient Particulate Matter Removal**. ACS Nano, 11 (6) (2017), pp. 6211-6217.

110. Feng, Y., et al., **Self-Powered Electrostatic Filter with Enhanced Photocatalytic Degradation of Formaldehyde Based on Built-in Triboelectric Nanogenerators**. ACS Nano, 11 (12) (2017), pp. 12411-12418.

111. Han, C.B., et al., **Removal of Particulate Matter Emissions from a Vehicle Using a Self-Powered Triboelectric Filter**. ACS Nano, 9 (12) (2015), pp. 12552-12561.

112. Liu, G., et al., **Self-Powered Electrostatic Adsorption Face Mask Based on a Triboelectric Nanogenerator**. ACS Applied Materials & Interfaces, 10 (8) (2018), pp. 7126-7133.

113. Mo, J., et al., **Radial piston triboelectric nanogenerator-enhanced cellulose fiber air filter for self-powered particulate matter removal**. Nano Energy, 78 (2020), pp. 105357.

114. Gu, G.Q., et al., **Triboelectric nanogenerator enhanced multilayered antibacterial nanofiber air filters for efficient removal of ultrafine particulate matter**. Nano Research, 11 (8) (2018), pp. 4090-4101.

115. He, C. and Z.L. Wang, **Triboelectric nanogenerator as a new technology for effective PM2.5 removing with zero ozone emission**. Progress in Natural Science: Materials International, 28 (2) (2018), pp. 99-112.

116. Zhang, X., N. Smith, and A. Webb, **1 - Medical Imaging**, in Biomedical Information

Technology, D.D. Feng, Editor. Academic Press: Burlington, 2008, pp. 3-27.

117. Hu, Z., et al., **Deep learning for image-based cancer detection and diagnosis－A survey**. Pattern Recognition, 83 (2018), pp. 134-149.

118. Bera, K., et al., **Artificial intelligence in digital pathology — new tools for diagnosis and precision oncology**. Nature Reviews Clinical Oncology, 16 (11) (2019), pp. 703-715.

119. Sahiner, B., et al., **Deep learning in medical imaging and radiation therapy**. Medical Physics, 46 (1) (2019), pp. e1-e36.

120. Singal, A.G., et al., **Hepatocellular Carcinoma Screening Associated with Early Tumor Detection and Improved Survival Among Patients with Cirrhosis in the US**. The American Journal of Medicine, 130 (9) (2017), pp. 1099-1106.e1.

121. Favoriti, P., et al., **Worldwide burden of colorectal cancer: a review**. Updates Surg, 68 (1) (2016), pp. 7-11.

122. Le, D.T., et al., **PD-1 Blockade in Tumors with Mismatch-Repair Deficiency**. New England Journal of Medicine, 372 (26) (2015), pp. 2509-2520.

123. Sharma, A., et al., **Single-walled carbon nanotube based transparent immunosensor for detection of a prostate cancer biomarker osteopontin**. Analytica Chimica Acta, 869 (2015), pp. 68-73.

124. Schwalbe, N. and B. Wahl, **Artificial intelligence and the future of global health**. The Lancet, 395 (10236) (2020), pp. 1579-1586.

125. Chaudhary, K., et al., **Deep Learning–Based Multi-Omics Integration Robustly Predicts Survival in Liver Cancer**. Clinical Cancer Research, 24 (6) (2018), pp. 1248.

126. Wei, W., et al., **Cancer registration in China and its role in cancer prevention and control**. The Lancet Oncology, 21 (7) (2020), pp. e342-e349.

127. Yang, Y. and W. Gao, **Wearable and flexible electronics for continuous molecular monitoring**. Chemical Society Reviews, 48 (6) (2019), pp. 1465-1491.

128. Zhang, H., et al., **Triboelectric nanogenerator built inside clothes for self-powered glucose biosensors**. Nano Energy, 2 (5) (2013), pp. 1019-1024.

129. Tang, Q., et al., **Whirligig-inspired triboelectric nanogenerator with ultrahigh specific output as reliable portable instant power supply for personal health monitoring devices**. Nano Energy, 47 (2018), pp. 74-80.

130. Song, Y., et al., **Wireless battery-free wearable sweat sensor powered by human motion**. Science Advances, 6 (40), pp. eaay9842.

131. Hu, S., et al., **Superhydrophobic Liquid–Solid Contact Triboelectric Nanogenerator as a Droplet Sensor for Biomedical Applications**. ACS Applied Materials & Interfaces, 12 (36) (2020), pp. 40021-40030.

Meihua Chen is a radiation oncologist of Sichuan Cancer Hospital & Institute, Affiliated Cancer Hospital, School of Medicine, University of Electronic Science and Technology of China. She received her B.M. degree (2010) and M.D. degree (2016) from West China

Medical School of Sichuan University. Her research focuses on radiation oncology, precision medicine for cancer, and artificial intelligence.

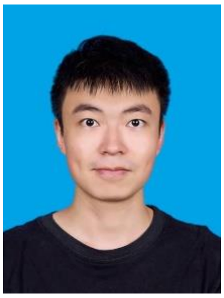

Yuankai Zhou obtained his B.S. in Applied Physics (2018) and M.S. in Electronic and Communication Engineering (2021) from University of Electronic Science and Technology of China. He is currently pursuing the Ph.D. degree under the guidance of Professor Yan Zhang in University of Electronic Science and Technology of China.

Jinyi Lang is a professor and the President of Affiliated Cancer Hospital, School of Medicine, University of Electronic Science and Technology of China, as well as the 8th Chairman of China Society for Radiation Oncology (CSTRO). He received his MD degree from Chongqing Medical University in 2003 and his B.M. from West China University of Medical Science, Sichuan, China, in 1983. His research interests include precision radiotherapy and telemedicine.

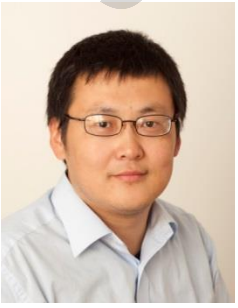

Lijie Li is a professor at Swansea University, UK. His research interests are design, modeling, fabrication, and characterization of MEMS, NEMS, sensors and actuators. He is Fellow of IET, and senior member of IEEE.

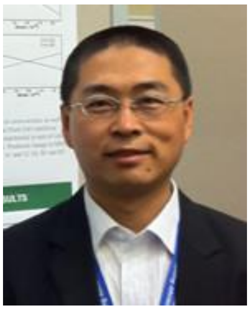

Yan Zhang is a professor at University of Electronic Science and Technology of China. He received his B. S. degree (1995) and Ph.D degree in Theoretical Physics (2004) from Lanzhou University. His research interests include self-powered nano/micro system, piezotronic and modeling of nonlinear dynamics of NEMS. He is senior member of IEEE.

Figure captions

Fig. 1. Schematic diagram of three ways to apply TENG device and AI algorithm to precise oncology. i. TENG as self-powered devices for cancer prevention, treatment and management; ii. TENG based self-powered sensor for collecting data on COA and non-COA measures for cancer; iii. The precise diagnosis and treatment of cancer using AI algorithm based TENG self-powered system.

Fig. 2. Application of TENG/PENG based self-powered devices for cancer treatment. (a) The structure of MTENG and the schematic diagram of it being applied for tumor treatment in mice. [35] (b) Workflow of the MTENG controlled drug delivery system. (c) Tumor samples taken from mice after 30 days. (d) The curve of mouse survival rate over time. (e) Structure diagram of the TENG based electroporation system. [48] (f) Structure diagram of the TENG electroporation drug delivery in vivo. [49] (g) Composition and working principle of s-PDT system based on ts-PENG. [46] (h) the curve of tumor size over time in different experiment groups. (i) Schematic diagram of the MP-Au/ZnO@CCM Trojan nanogenerators for tumor therapy. [52] (j) Survival rate of C6 cells in vitro experiment for 24 hours. (k) The curve of relative tumor volume over time in vivo in mice.

Fig. 3. Application of TENG based self-powered devices for tumor recovery. (a) Schematic illustration of the RD-TENG based electric stimulation system for wound healing. [61] (b) RD-TENG based electric stimulation system enhancing the migration behavior of L929 cells. (c) Schematic diagram of the mouse wearing the MSETENG to promote wound healing. [62] (d) Changes of wound area remaining in different groups of mice at different periods. (e) Schematic illustration of the iTENG patch for promoting wound healing and the mechanism for accelerating wound healing. [63] (f) Histogram of the wound area remaining in different groups of mice at different periods.

Fig. 4. Respiratory sensor for cancer patient management. (a) Schematic diagram of TENG powered SANES for respiratory monitoring and SANES structure. [65] (b) Flowchart of TENG based SANES collecting and processing abdominal respiratory behavior data. (c) Voltage signals produced by SANES under normal breathing, hypopnea and apnea. (d) The structure of the TENG in breath-based HMI system. [71] (e) The output features of TENG driven by different breathing behavior. (f) Schematic diagram of TENG driven breath-based HMI system controlling common electrical equipment. (g) Components of TENG based wireless HMI system. (h) Schematic diagram of wireless wearable sensor collecting respiratory behaviors data. [72] (i) Machine learning algorithm analyzes respiratory behaviors data from the sensor to predict subjects' posture.

Fig. 5. TENG based self-powered devices for UVR detection. (a) Structure of TENG based self-powered UV photodetector. [78] (b) The output current of the UV photodetector under different power intensities of UVR light. (c) Schematic diagram of the ENTENG structure and its working principle. [76] (d) Schematic diagram of UVR level detection system driven by ENTENG. (e) The output current of UVR sensor at different power intensities of UVR light.

Fig. 6. TENG based self-powered devices for ethanol detection. (a) Composition of the BD-TENG. [86] (b) Schematic diagram of BD-TENG as automatic alcohol breath analyzer. (c) Structure of the TENG driven ethanol sensor. [87] (d) The output current curve of the initial

ethanol sensor and the sensor enhanced by TENG at different concentrations of ethanol. (e) Response time, recovery time and response of the initial ethanol sensor and the TENG enhanced sensor. (f) Composition of the self-powered active sensor based on TENG. [88] (g) The response of the PTFE TENG under different ethanol concentration and Relative Humidity.

Fig. 7. The system based on sensors and machine learning algorithms for food-quality assessment. (a) Schematic diagram of TENG-based wireless gas sensor system. [101] (b) Response of conductive wood in TENG and TENG output voltage in air and ammonia. (c) The response of TENG in different concentrations of ammonia and the response of TENG in different gases with a concentration of 500 ppm. (d) The workflow of the electronic nose. [102] (e) The parameter scale and the accuracy of 1D-DCNN, ResNet-18 and RCSNN-12. (f) Schematic diagram of food quality estimation system based on radio frequency-powered sensor and machine learning algorithm. [103]

Fig. 8. TENG based self-powered device for air quality improvement. (a) Schematic diagram of TENG enhanced PM removal device and filtering mechanism of the filter. [109] (b) The removal efficiency of the initial filter and R-TENG enhanced filter when PM diameter is 15-550nm. (c) The removal efficiency of the initial filter and filter enhanced with R-TENG when PM diameter is 0.54-20μm. (d) Curve of formaldehyde concentration over time with and without TENG. [110] (e) Working principle of triboelectric filter to remove PM from exhaust gas. [111] (f) PM collection efficiency of self-powered triboelectric filter under different vehicle working modes. (g) The working principle of R-TENG during inhalation and exhalation, and the schematic diagram of SEA-FM. [112] (h) Removal efficiency of the PVDF-ESNF and R-TENG enhanced PVDF-ESNF.

Fig. 9. Cancer diagnosis based on AI algorithm and cancer marker sensor. (a) Schematic diagram of Tumor Origin Assessment via Deep Learning [39]. (b) Convolutional neural network based tumor detector. [40] (c) Another convolutional neural network based tumor classifier to classify MSI versus MSS. (d) Human labeled cancerous regions. [41] (e) Heatmaps generated by deep learning model. (f) Schematic diagram of deep learning model predicting outcome of

colorectal cancer [44] (g) Schematic diagram of PCa screening system based on multi-marker sensor and machine learning algorithm. [45] (h) Structure of SWCNT based osteopontin sensors. [123] (i) The curve of the relative resistance of the immunosensor varies with osteopontin concentration.

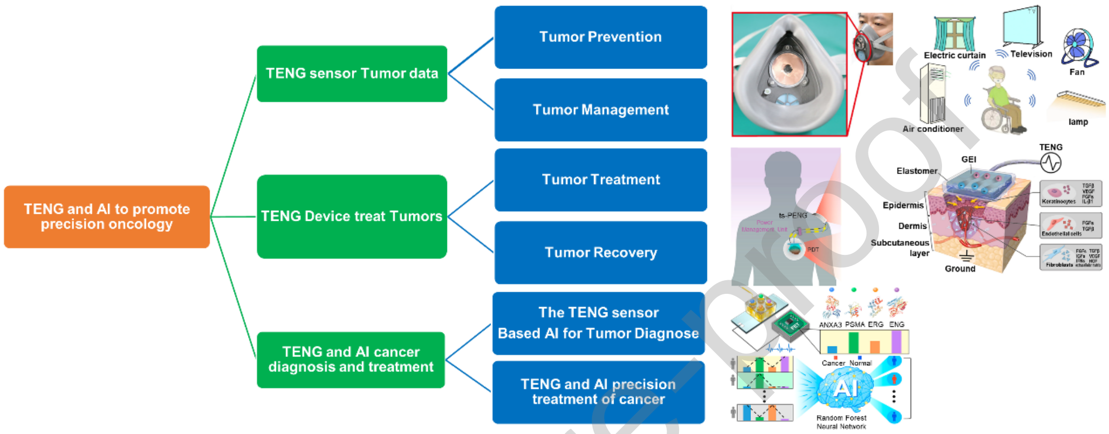

Fig. 1

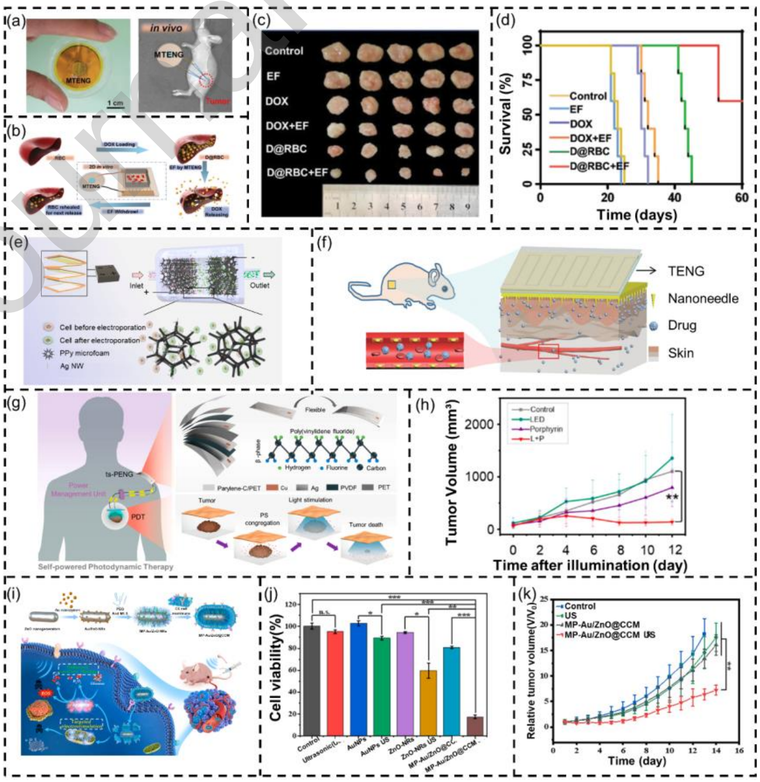

Fig. 2

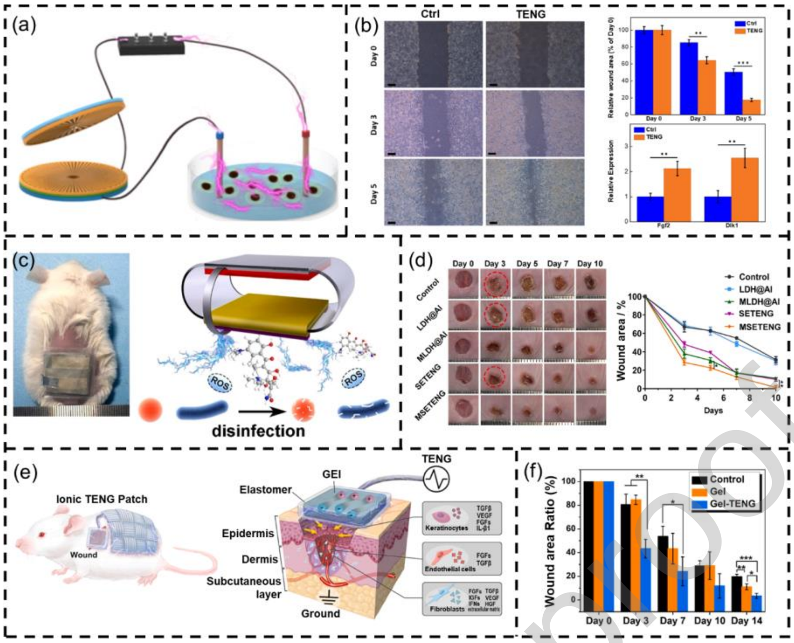
(a)
(b)
Ctrl
TENG
Day 0
Day 3
Day 5
(c)
disinfection
ROS
(d)
Day 0
Day 3
Day 5
Day 7
Day 10
Control
LDH@Al
MLDH@Al
SETENG
MSETENG
Wound area / %
Days
(e)
Ionic TENG Patch
Wound
TENG
GEI
Elastomer
Epidermis
Dermis
Subcutaneous layer
Ground
Keratinocytes
Endothelial cells
Fibroblasts
(f)
Wound area Ratio (%)
Control
Gel
Gel-TENG
Day 0
Day 3
Day 7
Day 10
Day 14

Fig. 3

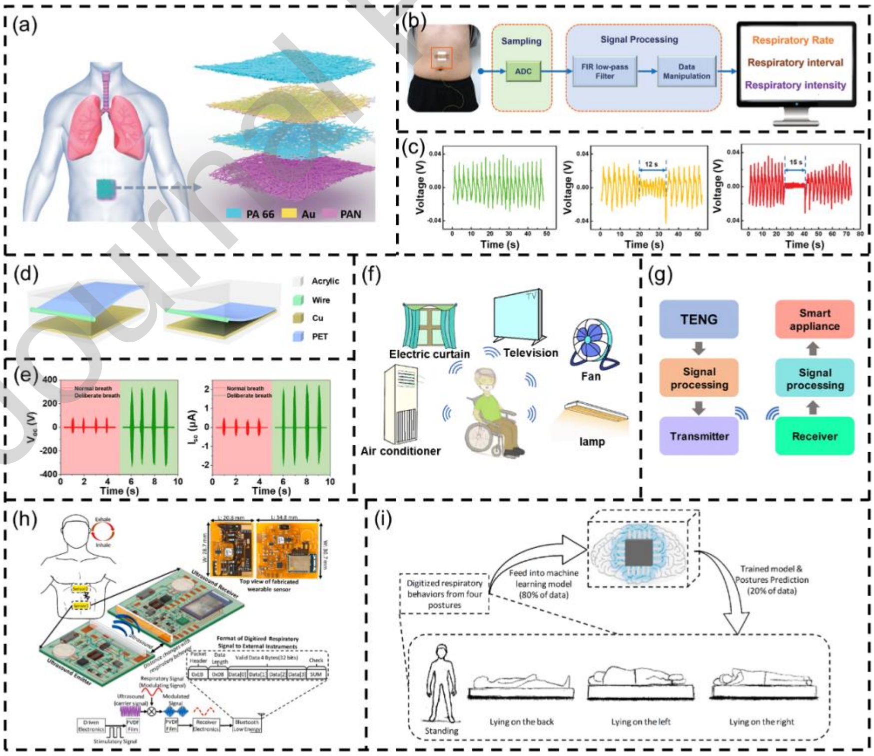
(a)
PA 66
Au
PAN
(b)
Sampling
ADC
Signal Processing
FIR low-pass Filter
Data Manipulation
Respiratory Rate
Respiratory interval
Respiratory intensity
(c)
Voltage (V)
Time (s)
12 s
15 s
(d)
Acrylic
Wire
Cu
PET
(e)
Normal breath
Deliberate breath
Time (s)
(f)
Electric curtain
Television
Fan
Air conditioner
lamp
(g)
TENG
Signal processing
Transmitter
Smart appliance
Signal processing
Receiver
(h)
Top view of fabricated wearable sensor
(i)
Digitized respiratory behaviors from four postures
Feed into machine learning model (80% of data)
Trained model & Postures Prediction (20% of data)
Standing
Lying on the back
Lying on the left
Lying on the right

Fig. 4

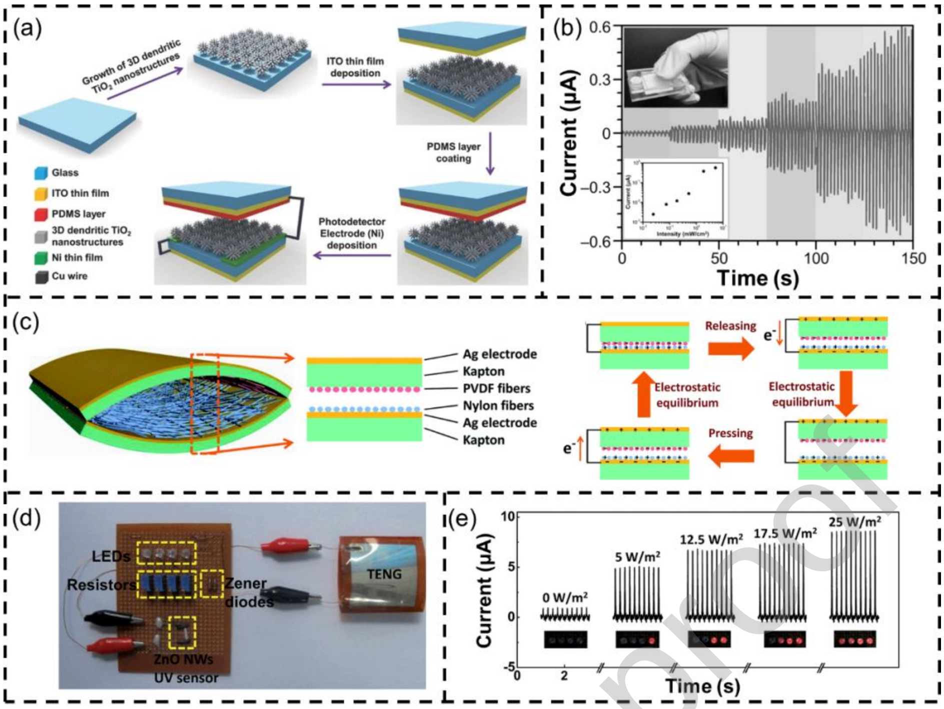
(a)
Growth of 3D dendritic TiO2 nanostructures
ITO thin film deposition
PDMS layer coating
Photodetector Electrode (Ni) deposition
Glass
ITO thin film
PDMS layer
3D dendritic TiO2 nanostructures
Ni thin film
Cu wire
(b)
Current (μA)
Time (s)
(c)
Ag electrode
Kapton
PVDF fibers
Nylon fibers
Ag electrode
Kapton
Releasing
Electrostatic equilibrium
Electrostatic equilibrium
Pressing
(d)
LEDs
Resistors
Zener diodes
TENG
ZnO NWs UV sensor
(e)
0 W/m2
5 W/m2
12.5 W/m2
17.5 W/m2
25 W/m2
Current (μA)
Time (s)

Fig. 5

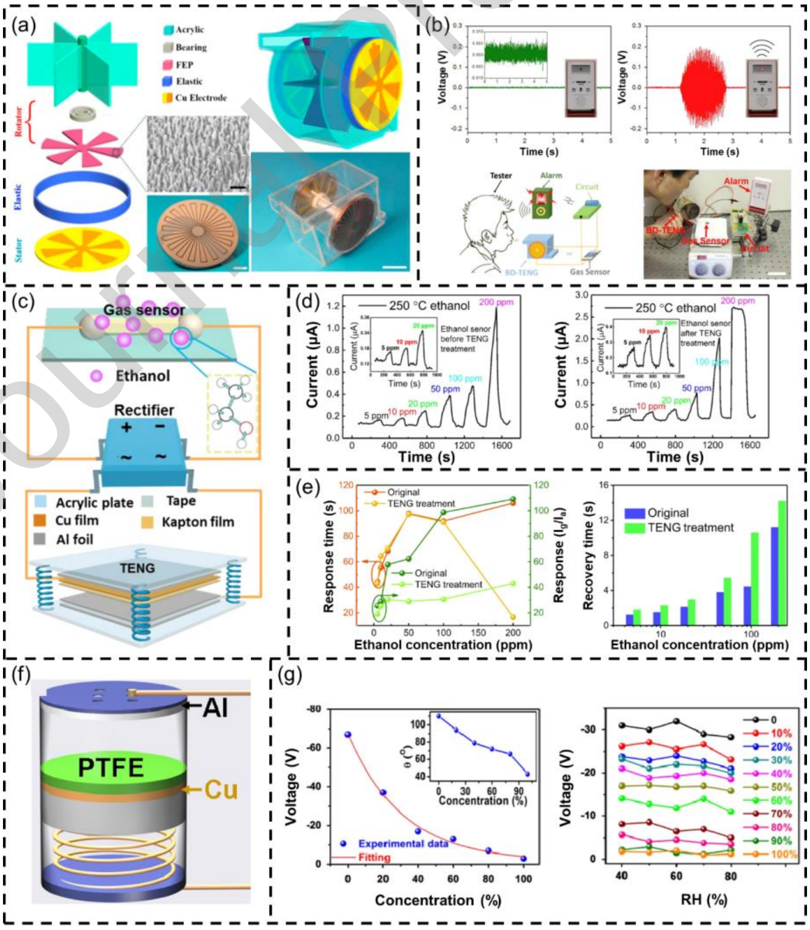
(a)
Acrylic
Bearing
FEP
Elastic
Cu Electrode
Rotator
Elastic
Stator
(b)
Voltage (V)
Time (s)
Tester
Alarm
Circuit
BD-TENG
Gas Sensor
(c)
Gas sensor
Ethanol
Rectifier
Acrylic plate
Tape
Cu film
Kapton film
Al foil
TENG
(d)
250 °C ethanol
Ethanol senor before TENG treatment
Ethanol senor after TENG treatment
5 ppm
10 ppm
20 ppm
50 ppm
100 ppm
200 ppm
Current (μA)
Time (s)
(e)
Original
TENG treatment
Response time (s)
Response (Ig/Ia)
Ethanol concentration (ppm)
Recovery time (s)
(f)
Al
PTFE
Cu
(g)
Voltage (V)
Experimental data
Fitting
Concentration (%)
RH (%)
0
10%
20%
30%
40%
50%
60%
70%
80%
90%
100%

Fig. 6

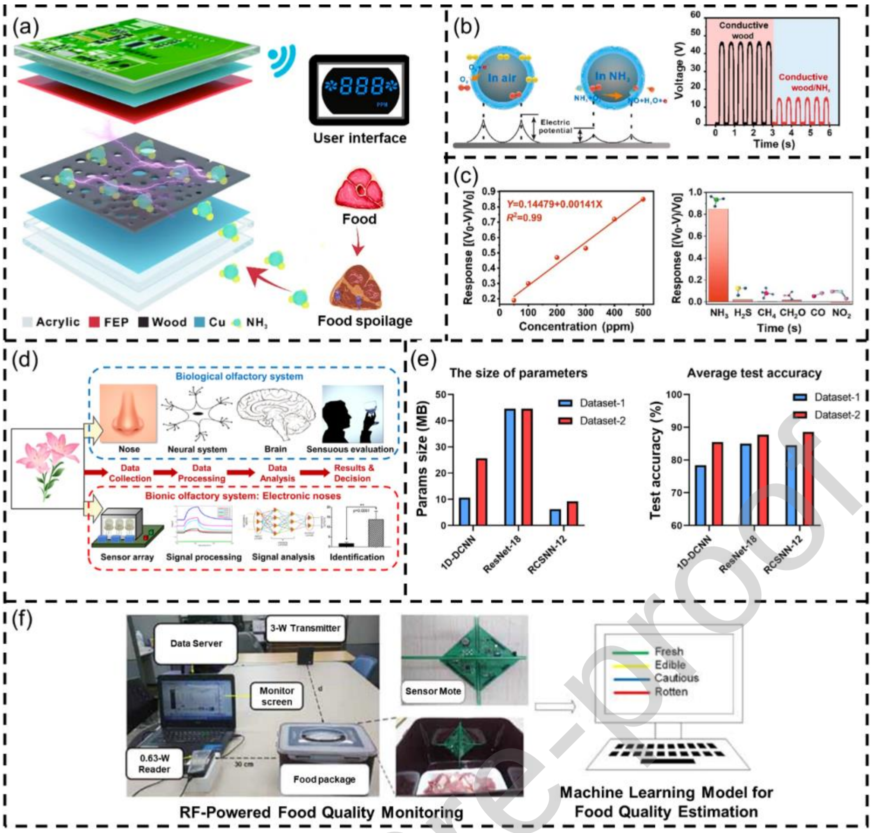
(a)
User interface
Food
Food spoilage
Acrylic FEP Wood Cu NH₃
(b)
In air
In NH₃
Electric potential
Conductive wood
Conductive wood/NH₃
Voltage (V)
Time (s)
(c)
Y=0.14479+0.00141X
R²=0.99
Response [(V0-V)/V0]
Concentration (ppm)
Time (s)
(d)
Biological olfactory system
Nose
Neural system
Brain
Sensuous evaluation
Data Collection
Data Processing
Data Analysis
Results & Decision
Bionic olfactory system: Electronic noses
Sensor array
Signal processing
Signal analysis
Identification
(e)
The size of parameters
Average test accuracy
Params size (MB)
Test accuracy (%)
Dataset-1
Dataset-2
1D-DCNN
ResNet-18
RCSNN-12
(f)
Data Server
3-W Transmitter
Monitor screen
0.63-W Reader
Food package
Sensor Mote
Fresh
Edible
Cautious
Rotten
RF-Powered Food Quality Monitoring
Machine Learning Model for Food Quality Estimation

Fig. 7

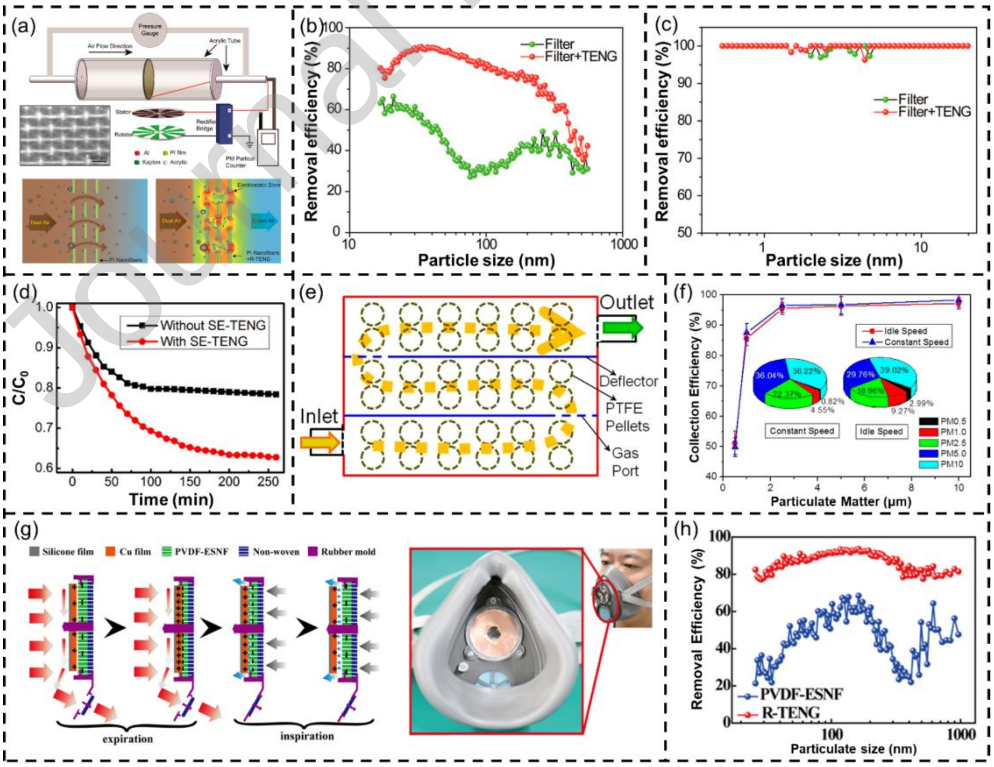
(a)
(b)
Removal efficiency (%)
Filter
Filter+TENG
Particle size (nm)
(c)
Removal efficiency (%)
Filter
Filter+TENG
Particle size (nm)
(d)
Without SE-TENG
With SE-TENG
C/C₀
Time (min)
(e)
Outlet
Inlet
Deflector
PTFE Pellets
Gas Port
(f)
Collection Efficiency (%)
Idle Speed
Constant Speed
Constant Speed
Idle Speed
PM0.5
PM1.0
PM2.5
PM5.0
PM10
Particulate Matter (μm)
(g)
Silicone film
Cu film
PVDF-ESNF
Non-woven
Rubber mold
expiration
inspiration
(h)
Removal Efficiency (%)
PVDF-ESNF
R-TENG
Particulate size (nm)

Fig. 8

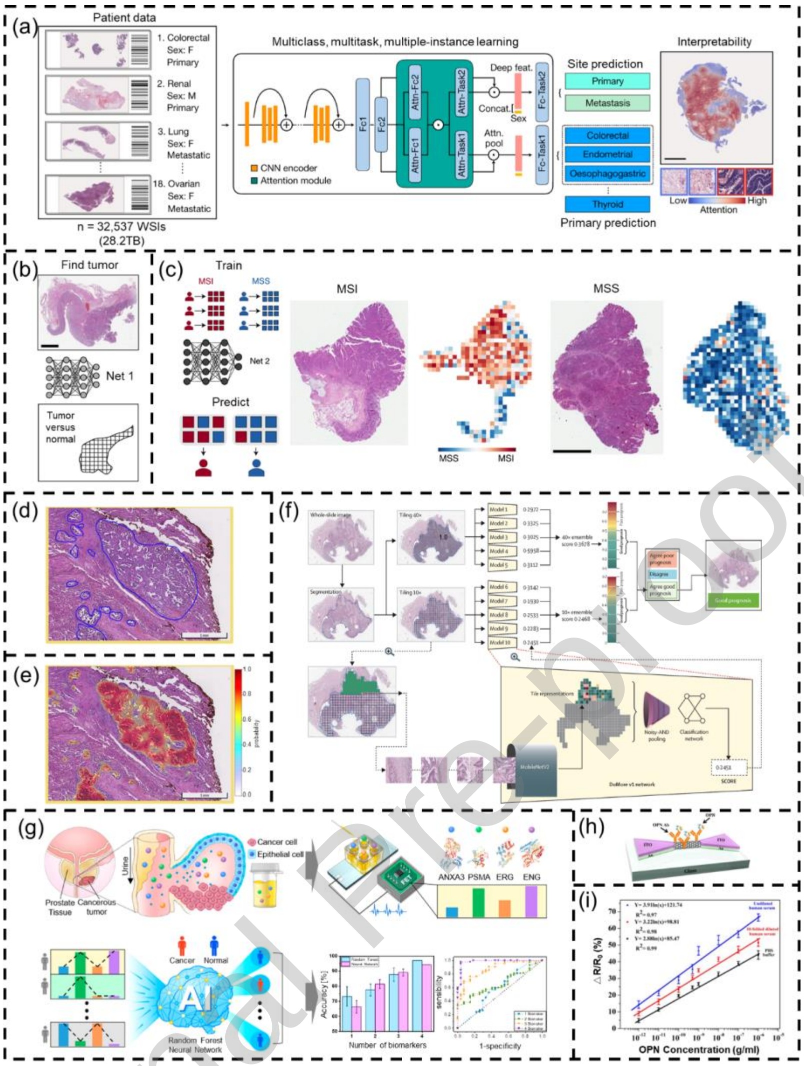

Fig. 9

CRediT authorship contribution statement

Meihua Chen: Conceptualization, Methodology, Formal analysis, Writing- Original draft preparation, Validation; **Yuankai Zhou:** Conceptualization, Methodology, Formal analysis, Writing- Original draft preparation, Validation; **Jinyi Lang:** Formal analysis, Validation; **Lijie Li:** Writing- Reviewing and Editing; **Yan Zhang:** Supervision, Conceptualization, Methodology, Formal analysis, Writing- Reviewing and Editing

Declaration of Competing Interest

☒ The authors declare that they have no known competing financial interests or personal relationships that could have appeared to influence the work reported in this paper.

☐The authors declare the following financial interests/personal relationships which may be considered as potential competing interests:

We wish to confirm that there are no known conflicts of interest associated with this publication and there has been no significant financial support for this work that could have influenced its outcome.

We confirm that the manuscript has been read and approved by all named authors and that there are no other persons who satisfied the criteria for authorship but are not listed. We further confirm that the order of authors listed in the manuscript has been approved by all of us.

We confirm that we have given due consideration to the protection of intellectual property associated with this work and that there are no impediments to publication, including the timing of publication, with respect to intellectual property. In so doing we confirm that we have followed the regulations of our institutions concerning intellectual property.

We understand that the Corresponding Author is the sole contact for the Editorial process (including Editorial Manager and direct communications with the office). He/she is responsible for communicating with the other authors about progress, submissions of revisions and final approval of proofs. We confirm that we have provided a current, correct email address which is accessible by the Corresponding Author and which has been configured to accept email from zhangyan@uestc.edu.cn

Signed by all authors as follows:

Graphical abstract

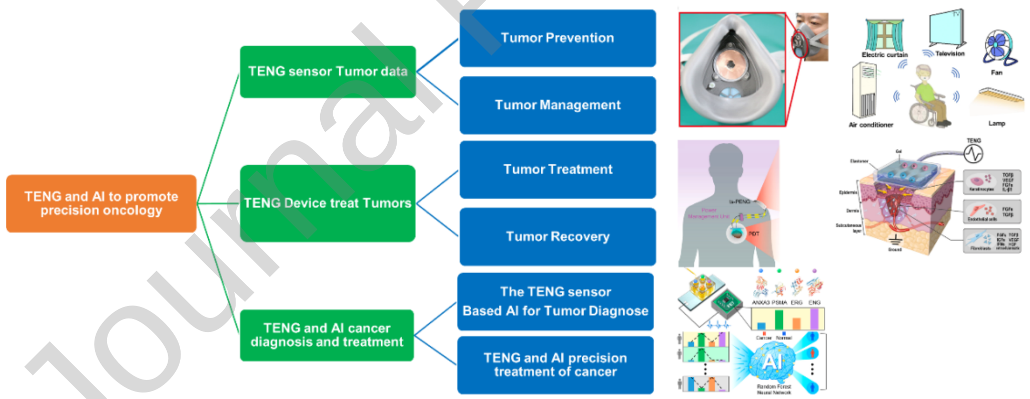

The applications of TENG for precision medicine in cancer. Wearable/implantable TENG/PENG and AI are key in timely data collection, data analysis, and feedback on the treatment. The integrated TENG and AI devices for early cancer diagnosis, precision cancer treatment, long-term patient data monitoring, and the TENG based AI system for cancer research.

Highlights

- TENGs based devices have been applied for targeted drug, photodynamic and electric field therapy on the cancer.
- TENGs with artificial intelligence have great potential in precision medicine in cancer diagnosis and treatment.
- The composition of self-powered devices and AI algorithms is essential for future precision medical in cancer.